

## Magnetic properties of the planar antiferromagnet $K_2FeF_4$

S. Mukhopadhyay and Ibha Chatterjee

*Saha Institute of Nuclear Physics, 92 Acharya Prafulla Chandra Road, Calcutta 700 009, India*

(Received 21 March 1984; revised manuscript received 3 July 1984)

Magnetic properties of the planar antiferromagnet  $K_2FeF_4$  have been studied using correlated-effective-field theory. Magnetic moments in this sample are confined in a plane due to an axial crystal field perpendicular to the plane. With the assumption that the magnetic moments lie in the  $x$  direction and the crystal-field anisotropy lies in the  $z$  direction, the sublattice magnetization and the susceptibilities are calculated and compared with experimental results. The exchange ( $J$ ) and the crystal-field ( $D$ ) parameters which give a best fit to the experimental results are  $J = -4.2 \text{ cm}^{-1}$  and  $D = 5.0 \text{ cm}^{-1}$ .

### I. INTRODUCTION

$K_2FeF_4$  is an example of planar antiferromagnets and it belongs to the  $K_2NiF_4$  family. While all other members of this family have a common property that their spins point parallel to the tetragonal  $c$  axis,  $K_2FeF_4$  has the peculiarity that the spins point perpendicular to the tetragonal  $c$  axis. Only very recently have its magnetic properties become fairly accurately known, and only a partial understanding of its magnetic data is available in the current literature. The compound  $K_2FeF_4$  has been investigated by many workers, who tried to probe various properties by different experimental methods. Thurlings *et al.*<sup>1</sup> measured the two-magnon Raman scattering and provided an estimate of the single-ion anisotropy. Macco *et al.*<sup>2</sup> measured the magnetic excitations and confirmed the presence of large anisotropy. Spin-wave dispersion and sublattice magnetization by the neutron scattering technique have been observed by Thurlings *et al.*<sup>3</sup> The temperature dependence of the magnetic excitation was measured by Balucani *et al.*<sup>4</sup> and the magnetic field behavior of the magnon mode was measured by Dürr and Schleeauf.<sup>5</sup> All these experiments reveal the two-dimensional character of this compound.

Direct measurements of the magnetization and the susceptibilities of this compound have become only recently available<sup>6,7</sup> from neutron scattering, NMR, and magnetometer experiments. In order to interpret the low-temperature magnetization data using renormalized spin-wave theory, Thurlings *et al.*<sup>6</sup> assumed  $J = -15.7 \pm 0.3 \text{ K}$ ,  $D = 5.7 \pm 0.1 \text{ K}$ , and  $E = -0.49 \pm 0.03 \text{ K}$ , while they obtained  $J = -16.4 \pm 0.3 \text{ K}$ ,  $D = 4.3 \pm 0.1 \text{ K}$ , and  $E = -0.29 \pm 0.03 \text{ K}$  to explain the Raman scattering experiment<sup>8</sup> using unrenormalized spin-wave theory. Thurlings *et al.* first studied<sup>9</sup> the magnetization by a Mössbauer experiment with the objective of estimating the critical exponent ( $\beta$ ) by means of a power-law fitting of the magnetization curve. Later from neutron scattering experiments<sup>3,6</sup> they obtained the magnetization curve and found the critical exponent ( $\beta$ ) in the same way. Structural studies of this compound with the help of the Mössbauer technique<sup>10</sup> and neutron scattering experiment<sup>11</sup> show that  $K_2FeF_4$  is isomorphous with  $Rb_2FeF_4$ .

These investigations confirm that the magnetic moments in  $K_2FeF_4$  order antiferromagnetically below 70 K with the moments lying in the  $XY$  plane. It has tetragonal crystal structure identical to  $K_2MnF_4$  and  $K_2NiF_4$ , and the lattice parameters are found<sup>12</sup> to be  $a = 4.41 \text{ \AA}$  and  $c = 12.98 \text{ \AA}$  at room temperature. From Mössbauer studies, the hyperfine-split spectrum at 71 K confirms the divalent character of the Fe ion. From various estimates of the transition temperature of this compound, it has been observed that the transition temperature should lie between 60 and 68 K. Thurlings *et al.*<sup>1</sup> quoted the transition temperature to be 60 K, while from Mössbauer study<sup>9</sup> they reported the transition temperature to be  $67.2 \pm 0.3 \text{ K}$ . However, performing a neutron scattering experiment,<sup>6</sup> they reported the transition temperature to be  $63.0 \pm 0.3 \text{ K}$ .

Various attempts have been made to understand theoretically the magnetic behavior of  $K_2FeF_4$ , of which one can mention those of Balucani *et al.*<sup>13</sup> and Thurlings *et al.*<sup>6-8</sup> Balucani *et al.*<sup>13</sup> employed a Green-function technique and matching of matrix element (MME) approach, whereas Thurlings *et al.*<sup>6-8</sup> used the spin-wave theory. As regards the susceptibility curve, they explained<sup>6</sup> different regions by using different theoretical models. In order to reproduce the low-temperature susceptibilities, they used the spin-wave theory for longitudinal susceptibilities and the molecular field theory for transverse susceptibilities. The high-temperature susceptibilities were reproduced by using the high-temperature series-expansion method. In this paper, we will attempt to account for the low-temperature as well as the high-temperature magnetic behavior using the correlated-effective-field (CEF) theory as developed by Lines.<sup>14</sup> The success of CEF theory in explaining the magnetic properties of low-dimensional compounds has already been examined.<sup>15</sup>

### II. THEORY

Correlated-effective-field theory goes beyond mean-field theory because static spin correlations are taken into account. This theory has been discussed in detail by Lines.<sup>14</sup> In this theory the CEF Hamiltonian becomes

$$\mathcal{H}_{\text{CEF}}^i = - \sum_{\gamma,j} J_{\gamma}^{ij} \alpha_{\gamma} (S_{\gamma}^i)^2 - 2 \sum_{\gamma,j} J_{\gamma}^{ij} S_{\gamma}^i (\langle S_{\gamma}^j \rangle - \alpha_{\gamma} \langle S_{\gamma}^i \rangle), \quad (1)$$

where  $i, j$  refer to the lattice sites and  $\gamma$  runs over the spatial components. All the lattice points are assumed to be equivalent in this theory. The order parameter is calculated from the equation

$$\langle S_{\lambda} \rangle = \frac{\sum_n \langle \psi_n | S_{\lambda} | \psi_n \rangle e^{-E_n/kT}}{\sum_n e^{-E_n/kT}}, \quad (2)$$

where  $\lambda$  is the direction of the easy axis.  $E_n$ 's are the eigenvalues obtained by diagonalizing the CEF Hamiltonian and  $|\psi_n\rangle$ 's are the corresponding eigenstates. The temperature-dependent correlation parameters ( $\alpha_{\gamma}$ ) are determined self-consistently from the equation

$$\alpha_{\gamma} = \sum_{\vec{q}} \frac{J_{\gamma}(\vec{q})kT}{kT - 2[J_{\gamma}(\vec{q}) - \alpha_{\gamma}J_{\gamma}(0)]\langle S_{\gamma}^i : S_{\gamma}^i \rangle} \times \left[ \sum_{\vec{q}} J_{\gamma}(0) \right]^{-1}. \quad (3)$$

This is computationally more convenient than the expression used by Lines.<sup>14</sup> The  $q$ -dependent susceptibilities are given by

$$\chi_{\gamma}(\vec{q}) = \frac{Ng^2\mu_B^2 \langle S_{\gamma}^i : S_{\gamma}^i \rangle}{kT - 2[J_{\gamma}(\vec{q}) - \alpha_{\gamma}J_{\gamma}(0)]\langle S_{\gamma}^i : S_{\gamma}^i \rangle}, \quad (4)$$

where  $\langle S_{\gamma}^i : S_{\gamma}^i \rangle$  has the usual meaning given by Lines.<sup>14</sup> From this equation the uniform molar susceptibility is calculated by setting  $\vec{q} = 0$ .

In the compound of interest  $\text{Fe}^{2+}$  has the electronic configuration  $3d^6$  and  ${}^5T_2$  is the ground-state term in the cubic field. Since there is a tetragonal distortion in the sample,  ${}^5T_2$  again splits up into a doublet  ${}^5E$  and a singlet  ${}^5B_2$  with  ${}^5B_2$  lying lowest. From a Mössbauer experiment this splitting has been found to be<sup>16</sup>  $\sim 700$  K and in our calculation only the ground-state term  ${}^5B_2$  is considered.  ${}^5B_2$  is orbitally nondegenerate and it is a spin-quintet state. The spin degeneracy can be lifted by the combined effect of tetragonal crystal field and spin-orbit interaction. This is incorporated in our theory by introducing a term  $D(S_z^i)^2$  in the spin Hamiltonian [Eq. (1)]. Further, an antiferromagnetic ordering demands that the nearest neighbors of an up spin at the  $i$ th site are all down spins, so that  $\langle S_{\gamma}^i \rangle = -\langle S_{\gamma}^i \rangle$ . Thus for planar antiferromagnets (four nearest neighbors) considering isotropic exchange interaction, our Hamiltonian becomes

$$\mathcal{H}^i = D(S_z^i)^2 - 4J[\alpha_x(S_x^i)^2 + \alpha_y(S_y^i)^2 + \alpha_z(S_z^i)^2] + 8JS_x^i \langle S_x^i \rangle (1 + \alpha_x), \quad (5)$$

where the spin moments are assumed to be aligned in the  $x$  direction. By solving Eqs. (2), (3), and (5) self-consistently, the uniform molar susceptibility is calculated from

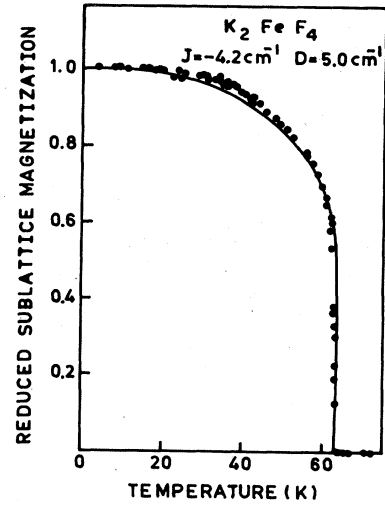


FIG. 1. Temperature dependence of the sublattice magnetization.

$$\chi_{\gamma}(0) = \frac{Ng^2\mu_B^2 \langle S_{\gamma}^i : S_{\gamma}^i \rangle}{kT - 2J_{\gamma}(0)(1 - \alpha_{\gamma})\langle S_{\gamma}^i : S_{\gamma}^i \rangle}. \quad (6)$$

### III. RESULTS AND DISCUSSION

Using the correlated-effective-field theory as discussed in Sec. II, the antiferromagnetic order parameter has been calculated and shown in Fig. 1. In this figure, the theoretical results are represented by a solid curve and the experimental results are denoted by dots. As our Hamiltonian contains two parameters ( $D$  and  $J$ ) only, the magnetic data are reproduced with a suitable choice of these two parameters. The best fit parameters are  $J = -4.2 \text{ cm}^{-1}$  and  $D = 5.0 \text{ cm}^{-1}$  which shows that the crystal field and the exchange interaction are of comparable magnitude. As evident from Fig. 1, an excellent agreement with experimental results is obtained with this set of parameters and our theoretical curve gives a correct estimate of the transition temperature<sup>6</sup> ( $T_N \sim 63$  K).

Using the same set of exchange and crystal-field parameters ( $J = -4.2 \text{ cm}^{-1}$ ,  $D = 5.0 \text{ cm}^{-1}$ ) and with  $g = 2$ , the

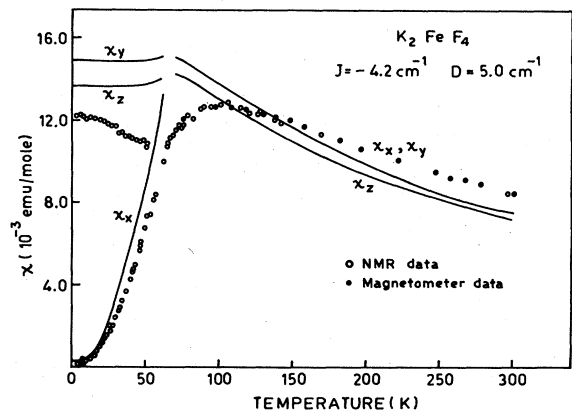


FIG. 2. Longitudinal ( $\chi_x$ ) and transverse ( $\chi_y, \chi_z$ ) susceptibilities as a function of temperature.

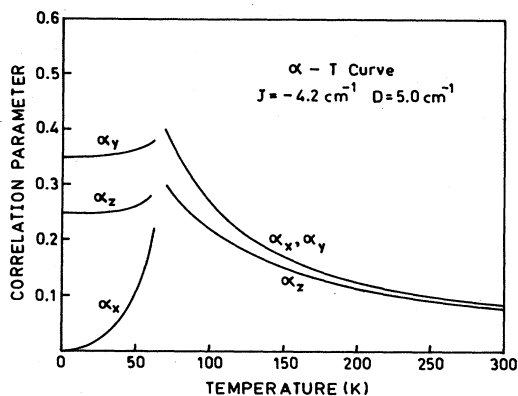


FIG. 3. Variation of correlation parameters with temperature.

susceptibilities in different directions ( $x, y, z$ ) are calculated in the temperature range 0–300 K. The theoretical results are shown by solid curves in Fig. 2 and these results are compared with the experimental results denoted by solid and open circles in the same figure. The solid circles represent the data obtained from magnetometer experiment and the open circles represent those obtained from NMR experiment. The variations of correlation parameters with temperature, as determined self-consistently in our calculations, are shown in Fig. 3. As Fig. 2 shows,

there is a qualitative agreement between the theoretical and the experimental results in the whole range of temperature 0–300 K and a quantitative agreement is found in the ordered phase only. The transverse susceptibilities in the ordered phase and the susceptibilities in the paramagnetic phase fail to agree quantitatively because in our calculation, only the crystal-field ground state  ${}^5B_2$  is considered. This is justified only in the calculation of longitudinal susceptibilities ( $\chi_x$ ) at low temperatures. In the calculations of  $\chi_y, \chi_z$  in the ordered phase and  $\chi$ 's in the paramagnetic phase, the excited crystal-field states which are supposed to be populated at higher temperatures should also be included. Therefore, if the mixing of low-lying excited states with the ground state due to spin-orbit and crystal-field effects is allowed, we hope, a quantitative agreement could be obtained. Figure 2 shows a small gap in the theoretical curve near the critical temperature. This is due to the fact that in a narrow region of temperature around  $T_N$ , we have not been able to find a self-consistent solution as numerical convergence is very poor in this region.

Although the two-dimensional character of  $K_2FeF_4$  is well established,<sup>6</sup> our present study also confirms this character. Therefore, we may conclude that CEF theory can not only explain the magnetic properties of three-dimensional compounds, but it explains the magnetic behavior of planar compounds as well.

- <sup>1</sup>M. P. H. Thurlings, A. van der Pol, and H. W. de Wijn, *Solid State Commun.* **24**, 829 (1977).
- <sup>2</sup>F. Macco, W. Lehmann, W. Breitling, A. E. Slawska Waniewska, R. Weber, and U. Dürr, *Solid State Commun.* **26**, 429 (1978).
- <sup>3</sup>M. P. H. Thurlings, E. Frikkee, and H. W. de Wijn, *J. Magn. Mater.* **15–18**, 369 (1980).
- <sup>4</sup>U. Balucani, M. G. Pini, and V. Tognetti, *J. Magn. Mater.* **15–18**, 371 (1980).
- <sup>5</sup>U. Dürr and O. Schleichauf, *Solid State Commun.* **35**, 847 (1980).
- <sup>6</sup>M. P. H. Thurlings, E. Frikkee, and H. W. de Wijn, *Phys. Rev. B* **25**, 4750 (1982).
- <sup>7</sup>M. P. H. Thurlings, B. J. Dikken, A. F. M. Arts, and H. W. de Wijn, *Phys. Rev. B* **25**, 4771 (1982).
- <sup>8</sup>M. P. H. Thurlings, A. van der Pol, and H. W. de Wijn, *Phys.*

- Rev. B* **25**, 4765 (1982).
- <sup>9</sup>M. P. H. Thurlings, E. M. Hendriks, and H. W. de Wijn, *Solid State Commun.* **27**, 1289 (1978).
- <sup>10</sup>G. K. Wertheim, H. J. Guggenheim, H. J. Levinstein, D. N. E. Buchanan, and R. C. Sherwood, *Phys. Rev.* **173**, 614 (1968).
- <sup>11</sup>R. J. Birgenau, H. J. Guggenheim, and G. Shirane, *Phys. Rev. B* **1**, 2211 (1970).
- <sup>12</sup>R. de Pape, *Bull. Soc. Chim. Fr.* 3489 (1965).
- <sup>13</sup>U. Balucani, M. G. Pini, and V. Tognetti, *J. Phys. C* **13**, 2925 (1980).
- <sup>14</sup>M. E. Lines, *Phys. Rev. B* **9**, 3927 (1974).
- <sup>15</sup>Ibha Chatterjee, *Physica (Utrecht) B&C* **104**, 403 (1981).
- <sup>16</sup>M. P. H. Thurlings, A. M. van Diepen, and H. W. de Wijn, *J. Magn. Mater.* **15–18**, 637 (1980).